Annals of Anatomy 240 (2021) 151855

Contents lists available at ScienceDirect

Annals of Anatomy

journal homepage: www.elsevier.com/locate/aanat

The long-term failure of RYGB surgery in improving T2DM is related to hyperinsulinism

Gonzalo-Martín Pérez-Arana[c,d,e,*], Alfredo Díaz Gómez[g], José Bancalero de los Reyes[a], Alonso Camacho-Ramírez[b], José Fernández-Vivero[c], Antonio Ribelles-García[c], David Almorza-Gomar[a,f], Carmen Carrasco-Molinillo[c], Isabel Mateo-Gavira[e,h], José-Arturo Prada-Oliveira[c,d,e,*]

[a] Complejo Hospitalario de Badajoz, Servicio Extremeño de Salud, Spain
[b] Surgery Unit, Puerta del Mar Universitary Hospital, University of Cadiz, Spain
[c] Department of Human Anatomy and Embryology, Faculty of Medicine, University of Cadiz, Spain
[d] Asociación Gaditana de Apoyo al Investigador (AGAI) Cádiz, Spain
[e] Institute for Bi omedical Science Research and Innovation (INIBICA) University of Cadiz, Spain
[f] Operative Statistic and Research Department, University of Cádiz, Spain
[g] San Carlos Hospital, Andalusian Health System, Spain
[h] Endocrine and Metabolic Unit, Puerta del Mar Universitary Hospital, University of Cadiz, Spain

ARTICLE INFO

Article history:
Received 5 July 2021
Received in revised form 2 November 2021
Accepted 3 November 2021
Available online 14 November 2021

Keywords:
Alpha-Cells
Beta-Cell mass
Pancreas
Type 2 Diabetes mellitus
Roux-en Y-gastric bypass
Incretins
Cellular differentiation

ABSTRACT

Background: Roux-en-Y gastric bypass (RYGB) is the gold standard method for bariatric surgery and leads to substantial improvements in Type 2 Diabetes mellitus. However, many patients experience relapses in diabetes five years after undergoing this aggressive surgical procedure. We focus on beta-cell population changes and absorptive intestinal consequences after RYGB in a healthy nonobese animal model after a long survival period.

Methods: For our purpose, we use three groups of Wistar rats: RYGB-operated, surgical control (Sham) and fasting control. We measure alpha-, beta-cell mass; transcription (Arx, and Pdx-1) and proliferation (Ki67) factors; glucose tolerance and insulin release after oral glucose tests; histological adaptive changes in the jejunum; and intestinal glucose transporters.

Results: Our results showed an early increase in insulin secretion after surgery, that decrease at the end of the study. The beta-cell mass reduces twenty-four weeks after RYGB, which coincides with decrease of Pdx-1 transcription promoter factor. These was coincident with an increase in alpha-mass and a high expression of Arx in RYGB group.

Conclusions: The analysis of all data showed beta-cell mass transdifferentiation into alpha-cell mass in RYGB rats. Due to long-term exhaustion of the beta-cell population by hyperinsulinism derived from digestive tract adaptation to surgery.

1. Introduction

Roux-en-Y gastric bypass (RYGB) has been determined to be a powerful therapy for improving obesity and Type 2 Diabetes mellitus (T2DM), even prior to weight loss (Pournaras et al., 2016). To explain this finding, many studies have reported increased GLP-1 plasma levels due to its enhanced release by L-cells in the ileum after surgery (Shah et al., 2014). This hormone has remarkable effects on beta-cell insulin secretion (Yabe and Seino, 2011) and beta-cell proliferation (Prada et al., 2019). However, the key role of GLP-1 in T2DM remission after glucose level restoration in GLP-1-deficient, diabetic, RYGB-operated mice is controversial (Mokadem et al., 2013). The peptide tyrosine-tyrosine (PYY), which is also secreted by L cells, has been proposed to be a key factor in glucose improvement after RYGB. PYY induces increased insulin and glucagon secretion from islets (Ramracheya et al., 2016).

RYGB also causes adaptive changes in the alimentary limb. These changes include long-term absorbent surface hypertrophy and

* Correspondence to: Department of Human Anatomy and Embryology, Faculty of Medicine, University of Cádiz, Plaza Fragela s/n Cádiz 11003, Spain.
E-mail addresses: gonzalo.perez@uca.es (G.-M. Pérez-Arana), arturo.prada@uca.es (J.-A. Prada-Oliveira).

https://doi.org/10.1016/j.aanat.2021.151855
0940-9602/

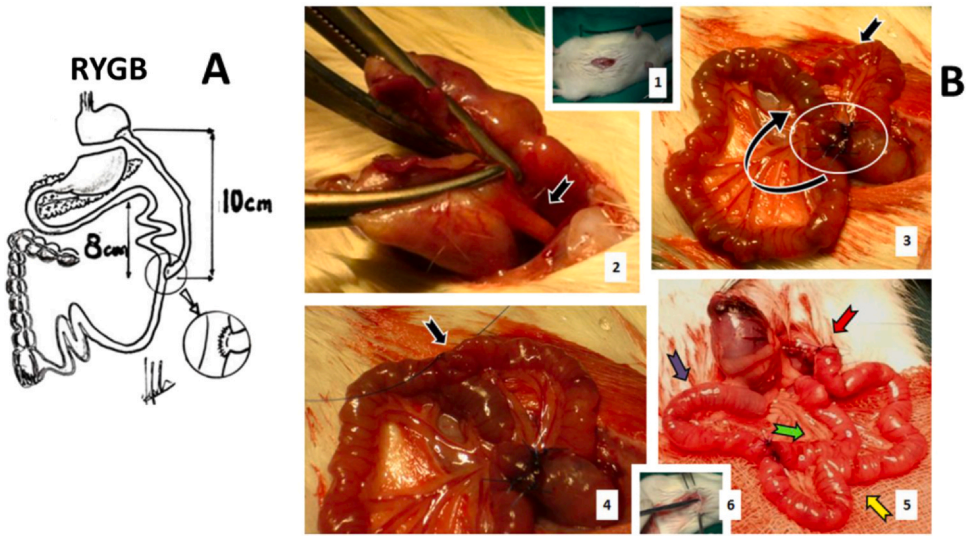

Fig. 1. **1**A. RYGB schema. **1**B. Surgical technique in RYGB. A laparotomy of 3 cm was performed in the midline of the abdomen (1), sectioning the gastrosplenic ligament (2) and exposing the stomach. A gastric pouch with a volume of approximately 30% of the normal gastric volume was created (3), and this pouch included the corpus and antrum (4). The remnant gastric fundus was anastomosed to the jejunum 14 cm distal from the ligament of Treitz (5).

increased glucose and protein absorption patterns (Seeley et al., 2015). These changes enhance the expression of glucose transporters, such as SGLT1, GLUT2, GLUT3, GLUT4 or GLUT5, in response to the loss of absorption area after surgery (Cavin et al., 2016).

These seem to suggest the physio-pathological basis for diabetes remission after RYGB. However, many RYGB patients experience reversal of T2DM improvement. Approximately 21.2–38.9% of patients present with T2DM relapse three years after surgery; the percentage of diabetes relapse reaches 33.1–50.8% five years after surgery (McTigue et al., 2020; Wang et al., 2020).

Many studies have reported a great plasticity of the beta–cell mass to dedifferentiate into alpha-cells under stressful conditions with high insulin requirements (Swisa et al., 2017). In these situations, beta-cells lose their markers, such as transcription insulin promoter factor (Pdx-1), or insulin production (Gao et al., 2014; Talchai et al., 2012). Instead, these cells express alpha-cell lineage markers, such as Aristaless-related homeobox protein (Arx).

We hypothesized that these factors could be involved in the instances of T2DM relapse after RYGB surgery. Beta-cell population plasticity with increased glucose uptake, as an adaptive response of the alimentary limb after RYGB, leads to a long-term condition of hyperinsulinemia. The reduced alimentary limb after surgery shortens the absorption surface, and consequently, the jejunum surface undergoes an adaptation process with elongated villi (Cavin et al., 2016). The consequence of these absorption peaks is a high demand for insulin release, which can lead to beta-cell exhaustion in the long-term (Abdel-Hamida and Firganya, 2019). Finally, RYGB could lead to a relapse of previously improved T2DM.

To this end, we used a nonobese healthy model of Wistar rats that underwent RYGB surgery. We analyzed the long-term beta-cell population response in order to explain T2DM relapse after RYGB. After surgery, we investigated histological and functional parameters after alimentary limb adaptation by measuring glucose transporter expression.

2. Material and methods

2.1. Animals and protocols

Thirty-six male Wistar rats weighing approximately 200–220 g and aged 10–11 weeks were provided by and housed at the Experimentation and Animal Production Service of University of Cádiz (SEPA). The animal procedures were performed with the approval of the University of Cádiz Committee for the Ethical Use and Care of Experimental Animals, and every experiment was performed in accordance with the relevant international guidelines and regulations related to animal welfare.

All the Wistar rats were randomly divided into three groups (n = 12 each): Fasting control (FG), Sham and Roux-en-Y gastric bypass (RYGB). Half of the animals (n = 6) in each of the three groups were sacrificed twelve weeks after surgery, and the remaining animals (n = 6) were sacrificed twenty-four weeks after surgery. The animals in the FG group (n = 12) underwent the same perioperative fasting periods described in the surgical protocol. All the animals finished a 12-h presurgical and 12-h postsurgical fasting period. An intake readaptation period followed the surgeries to normalize fasting. Weight was measured every three days beginning from the day of surgery until the fourth week of survival.

2.2. Surgical procedures: weight measurement

The surgical procedures were performed on anesthetized animals using a continuous infusion of isoflurane 2–4% V/V (Abbott Columbus, OH, USA). The sham technique (Sham) (n = 12) reproduced surgical damage near the intestine, but its integrity was maintained. Sham was performed with a laparotomy of 5 cm in the upper third of the abdomen and an incision of approximately 3 cm in the middle area of the abdomen. The jejunum was transected 40 cm distal to the angle of Treitz, with terminus-terminus anastomosis. The abdominal muscular and skin layers were closed in one layer using a continuous suturing technique.

In the RYGB group of rats (n = 12) were subjected to a pre- and postsurgical 12-hour fasting period. Animals were anesthetized with continuous infusion of 3% V/V isoflurane (Isoflo, Abbott 571329.8, Madrid, Spain). A laparotomy of 3 cm was made in the midline of the abdomen, and a gastric pouch with a volume of approximately 30% of the normal gastric volume was created (Fig. 1). The remnant gastric fundus was anastomosed to the jejunum at 14 cm distal from the ligament of Treitz. The abdominal muscular and skin layers were closed in one layer using a continuous suturing technique.

The weight gain of each animal in the three groups was measured every 48 h for forty days after surgery. The weight gain is expressed as medium daily weight gain in grams.

2.3. Oral glucose tolerance test (OGTT)

Three, eleven and twenty-three weeks after surgery, an oral glucose tolerance test (OGTT) was performed with the FC, Sham and RYGB groups. To this end, the animals were subjected to a 12-hour fasting period. A 20% v/v D-glucose solution (2 g/kg) was administered by gavage. Glycemia was measured by a Glucocard G-Meter 1810 glucometer (Menarini Diagnostics, Italy) in blood samples obtained from rat tails at 0, 30, 60, 90 and 120 min after glucose solution administration.

In each group, three, eleven and twenty-three weeks after surgery, insulin measurement was performed in blood samples obtained from the tails every 10 min for 60 min. For this oral glucose insulin test (OGIT), the rats were subjected to a 12-hour fasting period, and then, a glucose solution was administered. We used an ELIZA kit (ALPCO Diagnostics, Salem, NH, USA).

The area under the curve (AUC) was calculated according to the trapezoidal rule for both parameters.

2.4. D-Xylose absorption test

Eleven and twenty-three weeks after surgery, D-xylose absorption assay was performed in FC, Sham and RYGB. A D-xylose solution (0.8 g/kg body weigh) was administered through gavage, and plasma D-xylose levels were measured at 0, 60, 120 and 180 after load using spectrophotometric method as described Roe and Rice. Values obtained were expressed as D-xylose mmol/plasma ml.

Areas under curve (AUCs) were calculated by trapezoidal rule for each parameter in the study and expressed as plasma glucose mg/dl min-1, plasma insulin μU/ml min-1 and D-xylose mmol/ml min − 1.

2.5. Sacrifice and tissue preparation

Six animals from each group were sacrificed twelve weeks after surgery by isoflurane overdose via inhalation. The remaining 6 animals in the group were sacrificed twelve weeks later by isoflurane overdose via inhalation. Pancreas and gut samples were immediately removed and fixed in Bouin's solution overnight at 4 °C. Later, the samples were dehydrated, embedded in paraffin and cut into 8 μm microtome sections.

2.6. Pancreas immunostaining

Rehydrated sections of the pancreas, beta and alpha-cell masses were analyzed by immunostaining using guinea pig anti-insulin IgG antibodies (1/1000, Sigma Aldrich, St Louis MO, USA) and rabbit anti-glucagon IgG antibodies (1/5000, Abcam, Cambridge, CB4 OFL, UK). The fluorescent conjugated secondary antibodies (Alexa 546 and 488, 1/400 and 1/200 titers, respectively; Molecular Probes Inc. Eugene, OR, USA) were used. DAPI was used to counterstain the nuclei. Beta- and alpha-cell masses were calculated by multiplying the positive islet area/total pancreatic area ratio, by the total pancreatic weight (respectively, insulin- or glucagon- positive islet area). The results were expressed as milligrams (mg). These operation was performed three times in each animal and the results was expressed as the mean ± SEM.

The alpha-cell proliferation ratio was calculated by double immunostaining using rabbit anti-Ki67 IgG antibodies (1/50 titer, Abcam, Cambridge, CB4 OFL, UK) and mouse anti-glucagon IgG antibodies. The transcription factors Arx and Pdx-1 were also analyzed using rabbit anti-Arx IgG and rabbit anti-Pdx-1 antibodies (1/200 and 1/500, respectively; Abcam, Cambridge, CB4 OFL, UK). The fluorescent secondary antibodies were conjugated to Alexa 546 and 488 (1/400 and 1/200 titers, respectively, Molecular Probes Inc. Eugene, OR, USA). DAPI was used to counterstain the nuclei. Beta- and alpha-cell masses were calculated by multiplying insulin- or glucagon-positive area/total pancreatic area ratio/pancreatic weight, and the results are expressed as milligrams (mg).

The alpha-cell proliferation ratio was quantified in 50 islets per condition. The results were observed under randomized conditions by a single investigator and expressed as the number of glucagon-positive cells/Ki67-positive cells/mm^2 of the glucagon-positive area.

The numbers of Arx- and Pdx-1-positive cells per condition were evaluated in five nonserial slices of whole pancreas and expressed as the number of Arx- or PDX-1-positive cells/mm^2 of pancreas.

Using pancreas slices from the three animal groups, beta–cell apoptosis was determined using the Dead-End-Fluorometric terminal deoxynucleotidyltransferase-mediated 2´-deoxyuridine 5´-triphosphate nick end labeling system (TUNEL) (Promega, Madison, WI, USA) according to the manufacturer's instructions. Insulin was simultaneously stained using polyclonal guinea pig anti-insulin antibodies (Sigma-Aldrich, St Louis MO, USA). The fluorescent secondary antibodies were conjugated to Alexa 546 (1/400 titer, Molecular Probes Inc., Eugene, OR, USA). The apoptosis ratio was quantified in 30 islets per condition. The results were noted under randomized conditions by a single investigator and expressed as the number of TUNEL-positive and insulin-positive cells/mm^2 of islets.

2.7. Gut immunostaining and histological study

Ten nonserial rehydrated sections from the gut samples of each rat were analyzed by immunostaining using rabbit anti-SGLT1 IgG (1/500 titer, Abcam, Cambridge, CB4 OFL, UK), rabbit anti-GLUT1 IgG (1/200 titer, Bioss Inc., Woburn MA, USA) and rabbit anti-GLUT5 IgG (1/200 titer, Thermo-Fisher Inc., Burnaby, BC V5C 6S5, Canada). Samples from the intestinal tubes of the RYGB-operated rats were selected from the alimentary limbs, while samples from the equivalent part of the jejunum were collected from the Sham-operated rats group. The fluorescent secondary antibodies were conjugated to Alexa 546 and 488 (1/400 and 1/200 titers, respectively; Molecular Probes Inc. Eugene, OR, USA). DAPI was used to counterstain the nuclei. The values are expressed as SGLT-1-, GLUT1- or GLUT5-positive area/total intestinal area.

In addition, villus height and crypt depth were measured with eosin-hematoxylin-stained slices. Samples were selected from the alimentary limbs of the RYGB-operated animals or from equivalent parts of the jejunum of the Sham-operated animals. The values were expressed as length in μm. The histological parameters were measured and noted by a single investigator using a fluorescence microscope with a digital camera and Cell-D image analysis software (Olympus, GmbH. Hamburg, Germany).

2.8. Statistical analysis

The data are presented as the means ± SEM. For OGTT and insulin, AUC, histological and weight gain data analysis, one-way ANOVA followed by Tukey's/Bonferroni´s post hoc test was conducted using SPSS v21.0 software. Statistical significance was accepted at $P < 0.05$.

3. Results

3.1. Weight gain

We measured the weight gain in the FC, Sham and RYGB groups forty days after surgery (Fig. 2). There were no differences between any of the groups from the first day to the thirty-fourth day, but significant differences were observed between the control groups and the RYGB group beginning on the thirtieth day ($P < 0.05$) or from the thirty-second day to the end of the study ($P < 0.01$).

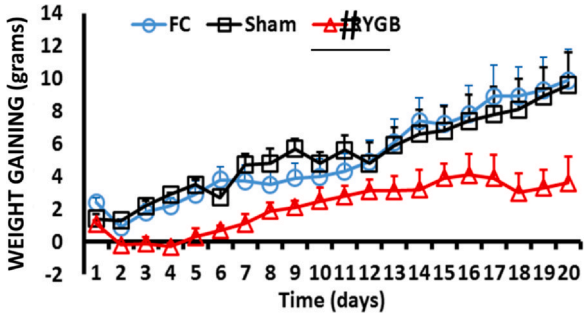

Fig. 2. Weight was measured every 48 h on each animal from n = 12 FC, n = 12 Sham and n = 12 RYGB groups, along forty days after surgery. It was expressed as medium daily weight gain in grams.

3.2. OGTT and OGIT

Three, eleven and twenty-three weeks after surgery, OGTT was performed on the animals in the FC, Sham and RYGB groups. Similar curves were observed in the three groups, with no significant differences between the glucose tolerance patterns of all the groups in the OGTT tests three and eleven weeks after surgery (Fig. 3A and 3B). However, a significantly high plasma glucose level in the RYGB group was observed (Fig. 3C). In the OGTT performed at twenty-three weeks after surgery, high glucose was observed thirty and sixty minutes after glucose administration (Fig. 3E). The area under the curve (AUC) was calculated for the three groups at three, eleven and twenty-three weeks after surgery. No significant differences between the FC, Sham and RYGB AUCs were found at the third or eleventh week (Figs. 3B and 3F). An increased AUC was observed in the RYGB-operated rats compared with the FC rats but not compared with the Sham rats at twenty–third weeks of survival (Fig. 3J).

Insulin secretion was analyzed after OGIT at the third, eleventh and twenty-third weeks of the study. A high plasma insulin secretion pattern was observed in the RYGB animals compared with both controls in the first and second OGIT tests (Fig. 3C and 3G). However, the RYGB insulin secretion pattern showed a significant decrease in the RYGB group compared to the control group in the last third test. The third OGIT was performed at the twenty-third week of survival (Fig. 3K). The insulin secretion AUCs after every OGIT were also measured. Increased AUC values were observed for the RYGB group compared with the control group after the first and second OGITs (Figs. 3D and 3H). However, the RYGB plasma insulin AUC was significantly decreased compared with the control plasma insulin AUC at twenty-three weeks after surgery, as shown in Fig. 3L.

3.3. D-Xylose absorption assay

Eleven and twenty-three weeks after surgery D–xylose absorption assay were performed on FC, Sham and RYGB groups. An increased absorption pattern appeared on RYGB curve respect to FC and Sham (Fig. 4A and 4C). Also significant increasing was observed between plasma D-xylose AUC from RYGB rats and controls at eleven and twenty-three weeks after surgery (Figs. 4B and 4D).

3.4. Pancreas immunostaining

The beta- and alpha-cell masses in the whole pancreas slices from the RYGB, FC or Sham rats were analyzed twelve and twenty-four weeks after surgery. The beta-cell mass exhibited a significant decrease between twelve and twenty-four weeks after surgery, as shown in Fig. 5A. Statistical differences appeared between the

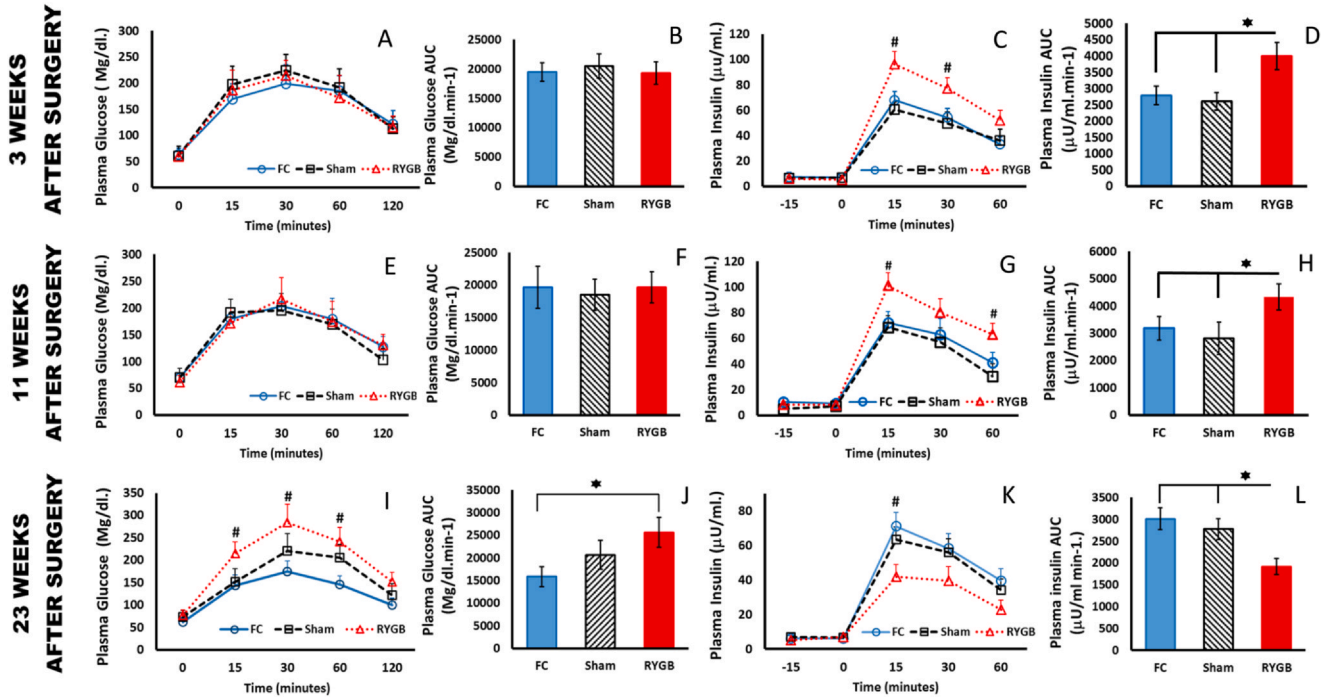

Fig. 3. 3A, 3E and 3L. Glucose levels, after the three OGTT, in fasting control (FC) (continuous blue line with circles), sham-operated (Sham) (discontinuous black line with squares), and RYGB rats (discontinuous red line with triangles). Glucose levels are represented as mg/dl in the Y axis versus time after glucose ingestion in the X axis. Values are expressed as the mean ± SEM. 3B, 3F and 3J. Glucose plasma area under curve (AUC) in fasting control (FC) (blue bar), sham-operated (Sham) (black lined bar), and RYGB rats (red bar), after the three OGTT. The values are presented as mg/dl min-1 in the Y axis, after the three OGTT, expressed as the mean ± SEM. 3C, 3G and 3K. Plasma insulin in fasting control (FC) (continuous blue line with circles), sham-operated (Sham) (discontinuous black line with squares), and RYGB rats (discontinuous red line with triangles), after the three OGTT. Plasma insulin levels are represented as µU/ml in the Y axis versus time after glucose ingestion in minutes in the X axis. Values were expressed as the mean ± SEM. 3D, 3H and 3L. Plasma insulin area under curve (AUC) in fasting control (FC) (blue bar), sham-operated (Sham) (black lined bar), and RYGB rats (red bar), after the three OGTT. The values were presented as µU/ml min-1 in the Y axis and expressed as the mean ± SEM.

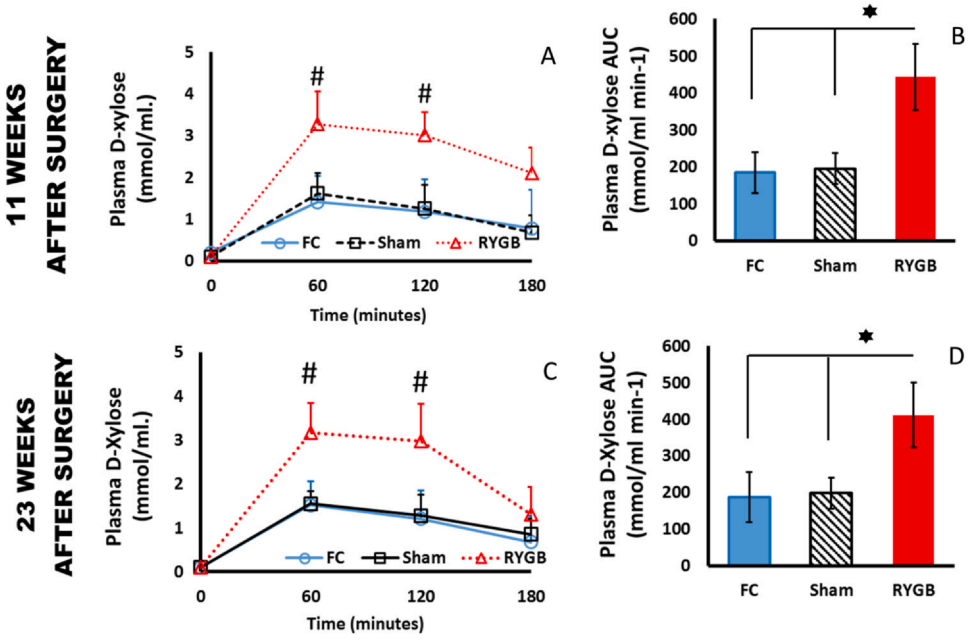

Fig. 4. 4.A. Plasma D-Xylose absorption assay insulin in fasting control (FC) (continuous blue line with circles), sham-operated (Sham) (discontinuous black line with squares), and RYGB rats (discontinuous red line with triangles), after eleven weeks after surgeries. Plasma D-xylose levels are represented as mmol/ml in the Y axis versus time after ingestion in minutes in the X axis. Values were expressed as the mean ± SEM. 4.B. Plasma D-xylose area under curve (AUC) in fasting control (FC) (blue bar), sham-operated (Sham) (black lined bar), and RYGB rats (red bar), after eleven weeks after surgeries. The values were presented as mmol/ml min-1 in the Y axis and expressed as the mean ± SEM. 4.C. Plasma D-Xylose absorption assay insulin in fasting control (FC) (continuous blue line with circles), sham-operated (Sham) (discontinuous black line with squares), and RYGB rats (discontinuous red line with triangles), after twenty-three weeks after surgeries. Plasma D-xylose levels are represented as mmol/ml in the Y axis versus time after ingestion in minutes in the X axis. Values were expressed as the mean ± SEM. 4.D. Plasma D-xylose area under curve (AUC) in fasting control (FC) (blue bar), sham-operated (Sham) (black lined bar), and RYGB rats (red bar), after twenty-three weeks after surgeries. The values were presented as mmol/ml min-1 in the Y axis and expressed as the mean ± SEM.

beta-cell mass of the RYGB animals twenty-four weeks after surgery and that of the control animals (Fig. 5A). On the other hand, at the twenty-fourth week of the study, we observed an increased alpha-cell mass in RYGB rats but not in any other group of rats (Fig. 5B).

We analyzed beta- and alpha-cell proliferation ratios in the FC, Sham and RYGB groups, twelve and twenty-four weeks after surgery. As a proliferation marker, we used the presence of Ki67 positive staining on beta- or alpha-cell populations (Fig. 6C and 6D). The results show a significant increase in the beta-cell proliferation ratio in the RYGB rat group twelve weeks after surgery compared with that in the RYGB groups twenty-four weeks after surgery ($P < 0.01$) and compared with that in the other groups in this study at every time ($P < 0.05$) No significant difference in the alpha-cell proliferation ratio was observed between the RYGB, Sham and FC groups at any time studied.

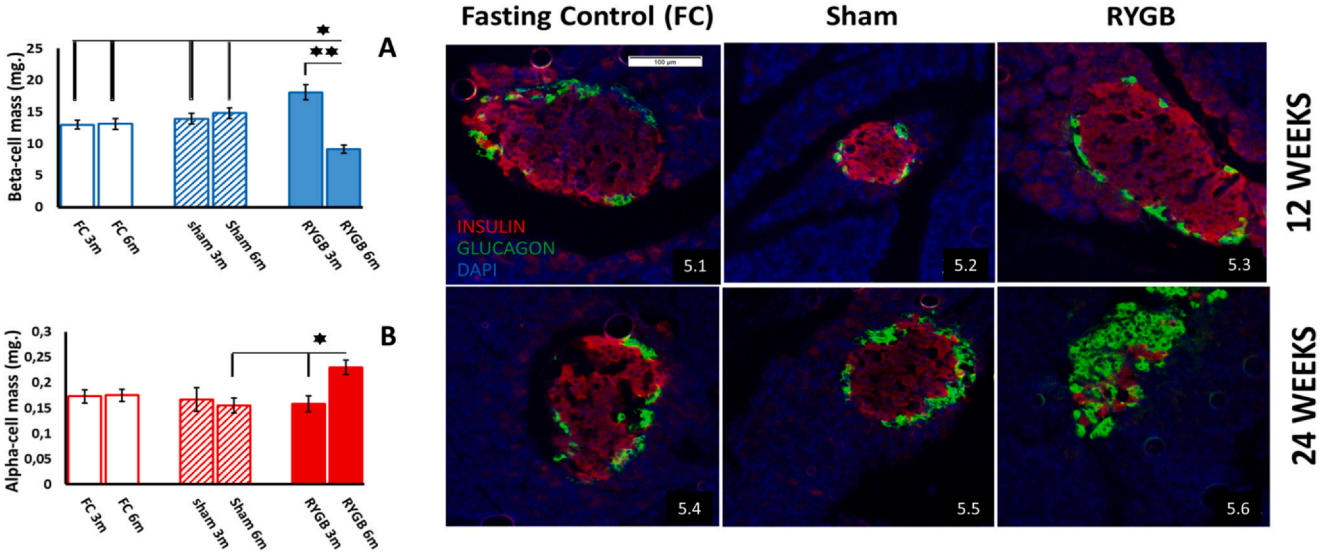

Fig. 5. Beta-cells in red, alpha cells in green (Alexa 546 and 488 respectively), and DAPI (blue) counterstained nuclei in FC (5.1 and 5.4, at 12 and 24 weeks after surgeries), Sham (5.2 and 5.5, at 12 and 24 weeks after surgeries) and RYGB (5.3 and 5.6, at 12 and 24 weeks after surgeries) in pancreas samples. 5A. Beta-cell mass expressed in milligrams (mg) in the Y axis, as the mean ± SEM in Fasting control (FC) (white bar), sham-operated (Sham) (lined bar), and RYGB rats (blue bar). The data show the two studied periods in the X axis. 5B. Alpha-cell mass expressed in milligrams (mg) in the Y axis, as the mean ± SEM in Fasting control (FC) (white bar), sham-operated (Sham) (lined bar), and RYGB rats (red bar). The data show the two studied periods in the X axis.

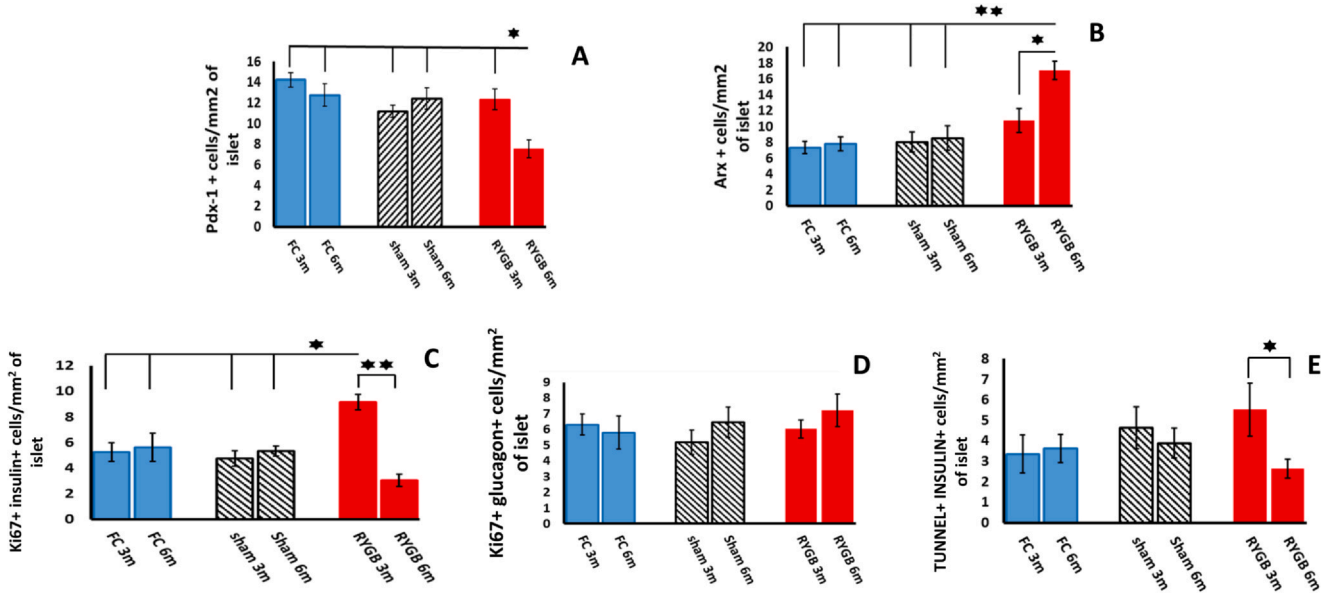

Fig. 6. 6A. Pdx-1 expression in beta-cell area as Pdx-1 + cells/mm^2 of insulin + area in the Y axis, as the mean ± SEM. Fasting control (FC) (blue bar), sham-operated (Sham) (lined bar) and RYGB rats (red bar). The data show the two studied periods in the X axis. 6B. Arx expression in beta-cell area as Arx+ cells/mm^2 of insulin+ area in the Y axis, as the mean ± SEM. Fasting control (FC) (blue bar), sham-operated (Sham) (lined bar) and RYGB rats (red bar). The data show the two studied periods in the X axis. 6C. Ki67 expression in beta-cell area as Ki67 + Insulin + cells/mm^2 of area in the Y axis, as the mean ± SEM. Fasting control (FC) (blue bar), sham-operated (Sham) (lined bar) and RYGB rats (red bar). The data show the two studied periods in the X axis. 6D. Ki67 expression in alpha-cell area as Ki67 + glucagon + cells/mm^2 of area in the Y axis, as the mean ± SEM. Fasting control (FC) (blue bar), sham-operated (Sham) (lined bar) and RYGB rats (red bar). The data show the two studied periods in the X axis. 6E. Apoptosis in beta-cell area as TUNNEL + Insulin + cells/mm^2 of area in the Y axis, as the mean ± SEM. Fasting control (FC) (blue bar), sham-operated (Sham) (lined bar) and RYGB rats (red bar). The data show the two studied periods in the X axis.

The Pdx-1 transcription factor, a differentiation marker in the beta-cell population, was measured by immunostaining. Loss of Pdx-1 expression was only detected in the RYGB-operated rat islets twenty–four weeks after surgery (Fig. 6A). These decreases were not observed at the twelfth week after surgery in either the FC or Sham groups at any time point. No other group at any time of the study or in RYGB at the initial period of study showed immunostaining in pancreatic islets.

Finally, the expression of Arx, an alpha-cell differentiation marker, was examined in the pancreas samples. Markedly increased cellular expression was observed in the RYGB group twenty-four weeks after surgery. However, no other group in this study exhibited Arx expression at any time (Fig. 6B).

The apoptosis beta-cell population ratio was measured twenty-four weeks after surgery in each group of the study using a Terminal deoxynucleotidyl transferase dUTP nick end labeling (TUNEL) assay. No significant difference was observed between the rats in the FC, Sham and RYGB groups (Fig. 6E).

3.5. Intestinal immunostaining

Several parameters, such as villus height, crypt depth or GLUT1, GLUT5 and SGLT1 expression, were measured in the intestinal tissue sections. Intestinal sections were selected from the alimentary limbs of the RYGB-operated rats. In the FC and Sham groups, the equivalent intestinal portion was the third proximal jejunum. These samples were obtained from the rats sacrificed both twelve and twenty-four weeks after surgery.

An increased villus height was observed in the alimentary limb samples from the RYGB rats at the two points in the study. These data were not observed in the FC or Sham groups at any time of the study (Fig. 7A). Crypt depth was also analyzed, and a strong development of crypts from the RYGB alimentary limb samples was observed but only at the final time point of the study, namely, twenty-four weeks after surgery. The FC and Sham groups did not show increased crypt depth development at any time (Fig. 7B).

Glucose transporter expression on the intestinal surface of the alimentary limbs from the RYGB rats or on the equivalent intestinal sections from the FC and Sham rats was also tested. The presence and degree of expression of SGLT1 was measured three and twenty-four months after surgery. High expression of SGLT1 was detected in the alimentary limb surface of the RYGB rats at twelve and twenty-four weeks compared with the FC or Sham rats at those time points. (Fig. 8A).

We also tested GLUT5 expression in each group. Markedly increased GLUT5 expression was observed twenty-four weeks, but not twelve weeks, after surgery in the alimentary limbs of the RYGB rats (Fig. 8B). No GLUT1 expression differences were observed between the equivalent intestinal segments in the FC and Sham groups at any time point (Fig. 8C).

4. Discussion

The present data show an interesting long-term effect of RYGB on glucose homeostasis in our model. In particular, the present data show an early increase in insulin secretion after surgery in the RYGB group compared with the control group at approximately twelve weeks after surgery, and this secretion decreased as the study progressed, reaching levels lower than those observed in the controls at the twenty-third week of the study (Fig. 3). This finding led us to consider an insulin secretory failure and a possible beta cell-population damage. That is why we investigated the beta-cell apoptosis ratio. However, no significant differences were observed among the groups (Fig. 6E). This finding is consistent with reports of the necessity of high plasma glucose levels to induce beta-cell apoptosis (Hui et al., 2004; Kim et al., 2005); because our model shows an early elevation of insulin secretion after RYGB and normal glycemia throughout most of the study. Surprisingly, the beta-cell mass was depleted twenty-four weeks after RYGB, as shown in Fig. 5A. The possibilities of beta-cell apoptosis and hepatic insulin resistance were excluded because Wistar rats are a healthy model. Few

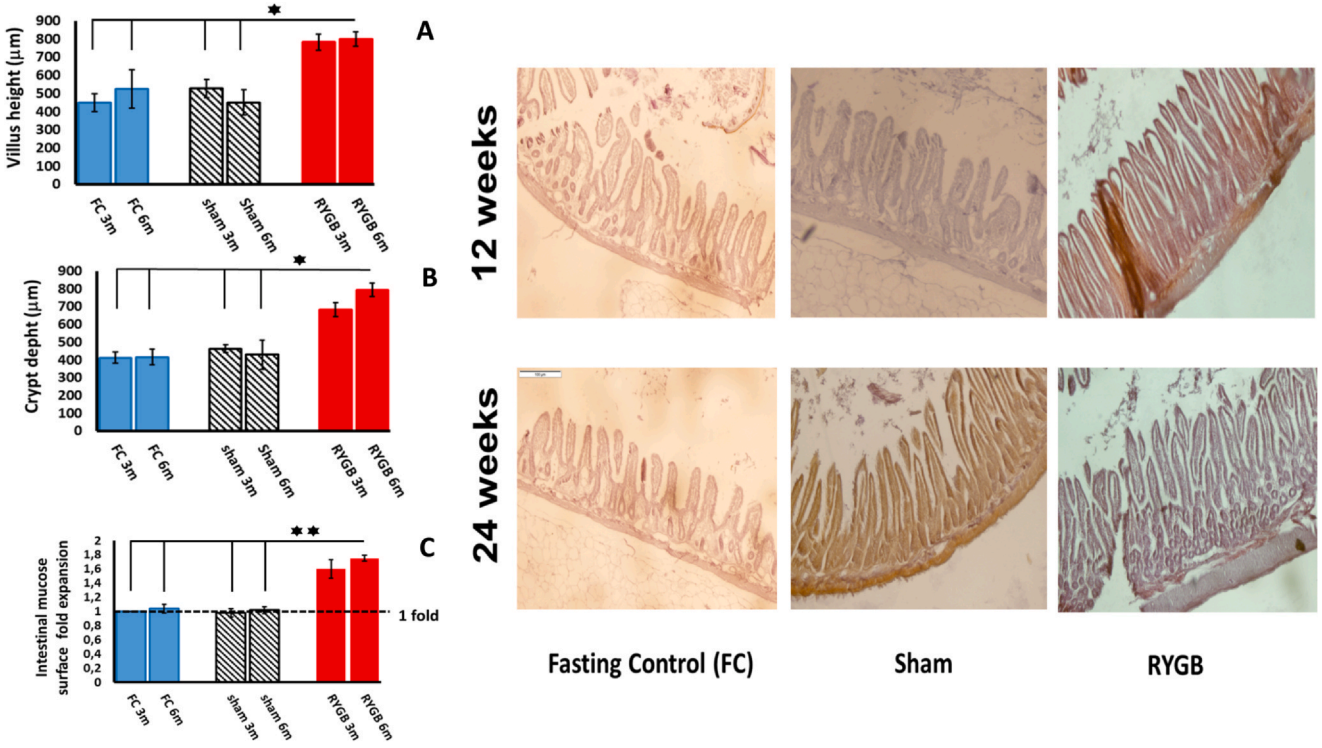

Fig. 7. Microphotograph of histologic studies. Left photos of FC (at 12 and 24 weeks after surgeries), middle photos of Sham (at 12 and 24 weeks after surgeries) and right photos of RYGB (at 12 and 24 weeks after surgeries) in jejunal samples. 7A. Villus weight of jejunal samples as µm in the Y axis, as the mean ± SEM. Fasting control (FC) (blue bar), sham-operated (Sham) (lined bar) and RYGB rats (red bar). The data show the two studied periods in the X axis. 7B. Crypt depth as µm in the Y axis, as the mean ± SEM. Fasting control (FC) (blue bar), sham-operated (Sham) (lined bar) and RYGB rats (red bar). The data show the two studied periods in the X axis. 7C. Ratio of superficial intestinal mucosae in the Y axis, as average differences since the FC measured at three months after surgeries. Fasting control (FC) (blue bar), sham-operated (Sham) (lined bar) and RYGB rats (red bar). The data show the two studied periods in the X axis.

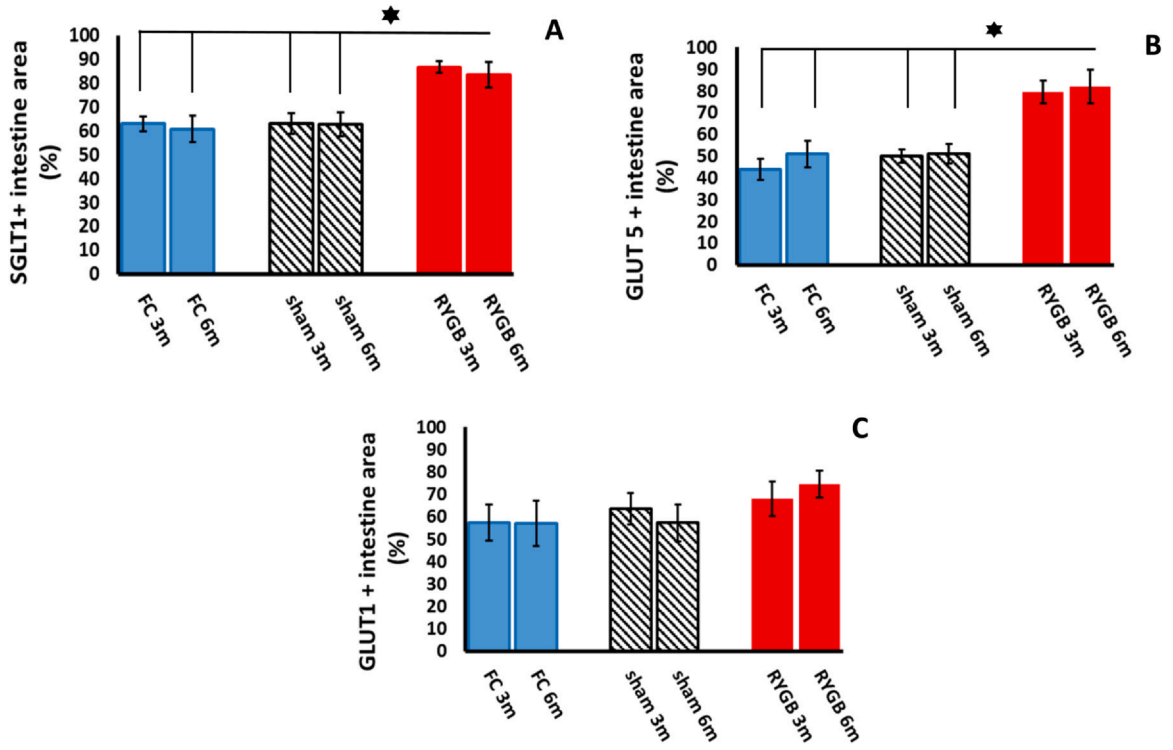

Fig. 8. 8A. SGLT1 Glucose transporter expression on the intestinal surface as SGLT1 + area/total intestinal area in the Y axis, as the mean ± SEM. Fasting control (FC) (blue bar), sham-operated (Sham) (lined bar) and RYGB rats (red bar). The data show the two studied periods in the X axis. 8B. GLUT5 Glucose transporter expression on the intestinal surface as GLUT5 + area/total intestinal area in the Y axis, as the mean ± SEM. Fasting control (FC) (blue bar), sham-operated (Sham) (lined bar) and RYGB rats (red bar). The data show the two studied periods in the X axis. 8C. GLUT1 Glucose transporter expression on the intestinal surface as GLTU1 + area/total intestinal area in the Y axis, as the mean ± SEM. Fasting control (FC) (blue bar), sham-operated (Sham) (lined bar) and RYGB rats (red bar). The data show the two studied periods in the X axis.

possibilities remain to explain the decreased insulin secretion and beta-cell mass loss throughout the study.

On the other hand, a decrease on the cell replication marker Ki67 was observed in beta cells from RYGB-operated animals six month after surgery (Fig. 6C). Discarding the proliferative mechanism as a cellular response to stress. This result opposes previous reports, which described the proposed proliferation as the principal response to a stressful situation (Dor et al., 2004). We must insist these experiences are based in different stressful situations.

In this way, many authors have proposed beta-cell dedifferentiation as a pathophysiological mechanism that leads to a loss of beta-cell mass in a few situations, as a high insulin requirement for a long time (Wang et al., 2014). To investigate possible beta-cell dedifferentiation, we tested the expression of a beta-cell marker, transcription insulin promoter factor (Pdx-1) in rodent groups (Segerstolpe et al., 2016; Henry et al., 2019). Pdx-1 islet expression declined in the RYGB rats at the late stage of the experiment (Fig. 6A). This data supports a long-term loss of beta-cell identity in animals after RYGB, which explains the loss of beta-cell mass and insulin secretion throughout the study. This mechanism seems to explain beta-cell failure in T2DM (Talchai et al., 2012).

In addition, an increase in alpha-cell mass was also observed at six, but not three, months after surgery in the RYGB rats (Fig. 5B). We exclude the possibility of an increased alpha-cell proliferation ratio (Fig. 6D). Thus, we considered beta-cell transdifferentiation more than beta-cell dedifferentiation in our model. Beta-cell transformation into alpha-cells has been reported as a consequence of beta-cell loss or insulin resistance in animal models (Tanday et al., 2020). Additionally, Pdx-1 activity is a repressor of the alpha-cell genetic program (Gao et al., 2014), and the normal proliferation ratio was observed in the alpha-cells from the RYGB rats.

Supporting our proposal, high expression of Aristaless-related homeobox protein (Arx) was observed in the RYGB group twenty-four weeks after surgery but not at twelve weeks after surgery (Fig. 6B). Arx protein is an alpha-cell differentiation marker, whose expression in beta-cells converts these cells into alpha- or PP-cells (Courtney et al., 2014; Segerstolpe et al., 2016; Bakhti et al., 2019; Henry et al., 2019).

Taken together, these data suggest a long-term beta-cell mass transdifferentiation into alpha-cell mass in RYGB rats, which can explain the loss of insulin secretion capacity at the end of the study. However, several questions remain uncertain. What factor that triggers this beta-cell response? Why does beta-cell transdifferentiation occur in the long term? It´s well known that there are beta-cells subpopulations with different characteristics and even identity markers (Avrahami et al., 2017). These subpopulations could not be equally affected after these differentiation process.

Analyzing the plasma insulin secretion in the RYGB group throughout the study, as we said above, an enhanced insulin secretion pattern at the early stage of the assay was observed (Fig. 3D). Thinking about the high plasma insulin secretion pattern as a response to high glucose absorption in the alimentary limb, we measured alimentary limb hypertrophy. The villus and crypt overgrowth from each group were compared, and a markedly higher villus height and a greater crypt depth were observed in the guts of the RYGB rats (Fig. 7). These data suggest a larger area for glucose absorption. To complete the study, sodium-glucose linked transporter (SGLT-1) and (GLUT-5) expression in the alimentary limbs was investigated. Statistical differences were observed in the glucose transporter densities between the control and RYGB groups at twelve and twenty-four weeks of the study (Fig. 8), confirming the results of Cavin et al. (2016).

An increased absorption surface and a high GLUT-5 and SGLT-1 density could justify significant glucose absorption in the gut after RYGB. This is supported by data shown at Figs. 3B and 3D, where we measured plasma levels of a non metabolizable-sugar as D-xylose. A high D-xylose absorption was observed in RYGB rats since the beginning of the study, instead of FC or Sham groups. In fact, this would explain the need for high plasma insulin levels to maintain normal postprandial glycemia after RYGB, as Fig. 3 show. The requirement of high levels of insulin secretion for a long time would lead to beta-cell population stress and transdifferentiation into alpha-cells. As beta-cell marker loss and alpha-cell marker gain were observed many weeks after RYGB (Fig. 5). The loss of insulin-producing cells would be responsible for the long-term decrease in insulin secretion and postprandial high plasma glucose AUC at the end of the study (Fig. 3K and 3L). These data suggest a progressive and adaptive phenomenon that results in hyperglycemia. This would explain the reason for long-term T2DM resolution failure after RYGB. However, there are substantial differences between the endocrine pancreas and intestine of rodents and humans, which suggests the need for additional research on this issue.

We report the mechanism that could explain the data reported in some patient five-ten years after underwent RYGB. These patient return to a diabetic status, which could be related to the anomalous glucose transport. This glucose absorption produces glycemic picks and hyperinsulinism. The consequence to this overload on beta-cells is a continuous stressful situation. Finally, stressed and exhausted beta-cell transdifferentiate to alpha-cell. This physiophathological mechanism needs to be confirmed in human clinic. But therefore, we could conclude that the RYGB might not be the desired treatment for some patients.

Authors contribution statement

A Camacho, G Pérez-Arana and JA Prada designed the project. D Almorza and J Bancalero analyzed the procedures for statistical analysis. A Diaz, J Bancalero, A Camacho, A Ribelles, C Carrasco, J Vivero and I Mateo performed the surgical techniques, followed the animal survival period and performed the functional test. G Pérez-Arana directed the histological techniques. All the authors participated in preparing the manuscript.

Declaration of Competing Interest

The authors declare that they have no known competing financial interests or personal relationships that could have appeared to influence the work reported in this paper.

Acknowledgments

The authors would like to thank the Asociacion Gaditana de Apoyo al Investigador *(AGAI),* Vice-Chancellor for Research Policies and INIBICA Institute for Biomedical Science Research and Innovation (INIBICA) University of Cadiz.

References

Abdel-Hamida, A.A., Firganya, A.L., 2019. Modulatory effect of empagliflozin on cellular parameters of endocrine pancreas in experimental pre-diabetes. Ann. Anat. 224, 153–160. https://doi.org/10.1016/jaanat.2019.05.002

Avrahami, D., Klochendler, A., Dor, Y., Glaser, B., 2017. Beta cell heterogeneity: an evolving concept. Diabetologia 60 (8), 1363–1369.

Bakhti, M., Bottcher, A., Lickert, H., 2019. Modelling the endocrine pancreas in health and disease. Nat. Rev. Endocrinol. 15 (3), 155–171.

Cavin, J.B., Couvelard, A., Lebtahi, R., Ducroc, R., Arapis, K., Voitellier, E., Cluzeaud, F., Gillard, L., Hourseau, M., Mikail, N., Ribeiro-Parenti, L., Kapel, N., Marmuse, J.P., Bado, A., Le Gall, M., 2016. Differences in alimentary glucose absorption and intestinal disposal of blood glucose after roux-en-y gastric bypass vs sleeve gastrectomy. Gastroenterology 150, 454–464.

Courtney, M., Rabe, T., Collombat, P., Mansouri, A., 2014. Pax4 and Arx represent crucial regulators of the development of the endocrine pancreas. New J. Sci. 2014, 1–6. https://doi.org/10.1155/2014/981569

Dor, Y., Brown, J., Martinez, O.I., Melton, D.A., 2004. Adult pancreatic beta cells are formed by self-duplication rather than stem-cell differentiation. Nature 429 (6987), 41–46.

Gao, T., McKenna, B., Li, C., Reichert, M., Nguyen, J., Singh, T., Yang, C., Pannikar, A., Doliba, N., Zhang, T., Stoffers, D.A., Edlund, H., Matschinsky, F., Stein, R., Stanger, B.Z., 2014. Pdx1 maintains beta cell identity and function by repressing an alpha-cell program. Cell Metab. 19, 259–271.

Henry, B.M., Skinningsrud, B., Saganiak, K., Pekala, P.A., Walocha, J.A., Tomaszewski, K.A., 2019. Development of the human pancreas and its vasculature – an integrated review covering anatomical, embryological, histological and molecular aspects. Ann. Anat. 221, 115–124. https://doi.org/10.1016/jaanat.2018.09.008

Hui, H., Dotta, F., Di Mario, U., Perfetti, R., 2004. Role of caspases in the regulation of apoptotic pancreatic islet beta-cells death. J. Cell. Physiol. 200 (2), 177–200.

Kim, W.H., Lee, J.W., Suh, Y.H., Hong, S.H., Choi, J.S., Lim, J.H., Song, J.H., Gao, B., Jung, M.H., 2005. Exposure to chronic high glucose induces beta-cell apoptosis through decreased interaction of glucokinase with mitochondria: downregulation of glucokinase in pancreatic beta-cells. Diabetes 54 (9), 2602–2611.

McTigue, K.M., Wellman, R., Nauman, E., Anau, J., Coley, R.Y., Odor, A., 2020. Comparing the 5-year diabetes outcomes of sleeve gastrectomy and gastric bypass: the national patient-centered clinical research network (PCORNet) bariatric study. JAMA Surg. 4, e200087. https://doi.org/10.1001/jamasurg.2020.0087

Mokadem, M., Zechner, J.F., Margolskee, R.F., Drucker, D.J., Aguirre, V., 2013. Effects of Roux-en-Y gastric bypass on energy and glucose homeostasis are preserved in two mouse models of functional glucagon-like peptide-1 deficiency. Mol. Metab. 3 (2), 191–201.

Pournaras, D.J., Nygren, J., Hagström-Toft, E., Arner, P., le Roux, C.W., Thorell, A., 2016. Improved glucose metabolism after gastric bypass: evolution of the paradigm. Surg. Obes. Relat. Dis. 12 (8), 1457–1465.

Prada-Oliveira, J.A., Camacho-Ramirez, A., Salas-Alvarez, J., Campos, F.J., Lechuga, A.L., Almorza-Gomar, D., Blandino-Rosano, M., Perez-Arana, G., 2019. GLP-1 mediated improvement of the glucose tolerance in the T2DM GK rat model after massive jejunal resection. Ann. Anat. 223, 1–7. https://doi.org/10.1016/jaanat.2019.01.007

Ramracheya, R.D., McCulloch, L.J., Clark, A., Johannessen, H., Olsen, M.K., Cai, X., Zhao, C.M., Chen, D., Rorsman, P., 2016. PYY-dependent restoration of impaired insulin and glucagon secretion in type 2 diabetes following Roux-En-Y gastric bypass surgery. Cell Rep. 15, 944–950.

Seeley, R.J., Chambers, A.P., Darleen, A., 2015. The role of gut adaptation in the potent effects of multiple bariatric surgeries on obesity and diabetes. Cell Metab. 21 (3), 369–378.

Segerstolpe, A., Palasantza, A., Eliasson, P., Andersson, E.M., Andreasson, A.C., Sun, X., Picelli, S., Sabirsh, S., Clausen, M., Magnus, K.B., Smith, D.M., Kasper, M., Ämmälä, C., Sandberg, R., 2016. Single-cell transcriptome profiling of human pancreatic islets in health and type 2 diabetes. Cell Metab. 24 (4), 593–607.

Shah, M., Law, J.H., Micheletto, F., Sathananthan, M., Dalla-Man, C., Cobelli, C., Rizza, R.A., Camilleri, M., Zinsmeister, A.R., Vella, A., 2014. Contribution of endogenous glucagon-like peptide 1 to glucose metabolism after Roux-en-Y gastric bypass. Diabetes 6, 483–493.

Swisa, A., Glaser, B., Dor, Y., 2017. Metabolic stress and compromised identity of pancreatic beta cells. Front. Genet. 8, 21. https://doi.org/10.3389/fgene.2017.00021

Talchai, C., Xuan, S., Lin, H.V., Sussel, L., Accili, D., 2012. Pancreatic beta cell dedifferentiation as a mechanism of diabetic beta cell failure. Cell 150, 1223–1234.

Tanday, N., Flatt, P.R., Irwin, N., Moffett, R.C., 2020. Liraglutide and sitagliptin counter beta- to alpha-cell transdifferentiation in diabetes. J. Endocrinol. 245, 53–64. https://doi.org/10.1530/JOE-19-0451

Wang, C., Zhang, H., Yu, H., Bao, Y., Zhang, P., Di, J., 2020. Roux-en-Y gastric bypass for T2DM treatment in chinese patients with low BMI: 5-year outcomes. Obes. Surg. Mar. 30, 2588–2597. https://doi.org/10.1007/s11695-020-04520-5

Wang, Z., York, N.W., Nichols, C.G., Remedi, M.S., 2014. Pancreatic beta cell dedifferentiation in diabetes and redi-erentiation following insulin therapy. Cell Metab. 19, 872–882.

Yabe, D., Seino, Y., 2011. Two incretin hormones GLP-1 and GIP: comparison of their actions in insulin secretion and b cell preservation. Prog. Biophys. Mol. Biol. 107 (2), 248–256.